Near-field optical microscope image formation: a theoretical and experimental study

A. V. Zvyagin

Tokyo Institute of Technology, Nagatsuta 4259, Yokohama 227, Japan

J. D. White

Kanagawa Academy of Science and Technology, Kawasaki, 213, Japan

M. Ohtsu

Tokyo Institute of Technology, Nagatsuta 4259, Yokohama 227, Japan, and Kanagawa Academy of Science and Technology, Kawasaki, 213, Japan

Received March 3, 1997

A quantitative comparison between theory and experiment has been carried out for a collection-mode near-field optical microscope. A 30-nm (lateral dimension) cylindrical dielectric sample was imaged. This image was compared with the result of theoretical calculations that used a classical macroscopic nonglobal model based on the excitation theorem. Good agreement was obtained, with image inversion, edge enhancement, and edge asymmetry correctly predicted. © 1997 Optical Society of America

The near-field optical microscope (NOM), a member of the family of scanning probe microscopes that includes the scanning tunneling microscope and the atomic force microscope, is different from other optical microscopes in that it exploits the unique properties of the optical near field to yield subwavelength resolution. As it does not harm the sample, it has found application in such diverse fields as biology, spectroscopy, and optical storage.[1] To gain insight into the NOM image-formation mechanism and to clarify the often puzzling relationship between NOM images and real topography that is encountered in experiments, it is important to specify inherent NOM phenomena to be studied both experimentally and theoretically. Such effects as spatial localization,[2,3] polarization-directional dependence,[4,5] and image inversion[2,6] can be attributed to these purely near-field effects. These effects are dominant in samples characterized by $kd \ll 1$ and $kh \ll 1$, where d is the width of the sample, h is the maximum height of the sample above the planar substrate, and k is the wave number of the light used in observing the specimen. (In the case of illumination with the commonly used red laser, $d, h \ll 100$ nm.) Samples that satisfy these criteria can be reasonably denoted near-field objects.[7] In the most recent of several initial attempts[8–10] to carry out both experimental and theoretical NOM image study, Weeber *et al.*[10] imaged a sample [$d = 100$ nm ($kd \sim 1$), $h = 70$ nm ($kh \sim 0.7$)] and found qualitative agreement with their microscopic theory.[2] In the present study we quantitatively compare experimental results with theoretical calculations based on a classical macroscopic nonglobal model, using a well-defined nanometric- [$d \sim 30$ nm ($kd \sim 0.3$), $h \sim 16$ nm ($kh \sim 0.15$)] sized dielectric sample.

Whereas the NOM can be operated in a number of different modes, we have chosen the collection-mode NOM (c-mode NOM) for this image-formation study because the polarization state of the incident light can be accurately controlled. In this configuration the sample is illuminated under the total-internal-reflection condition (Fig. 1) and the optical field probed by a sharpened fiber tip. An image is formed by detection of the changes in optical field intensity as the fiber is scanned laterally.

For modeling purposes the fiber tip apex is represented as a nanometer-sized dielectric sphere. As the probe and the sample interact weakly,[5] the intensity picked up by the probe is proportional to the near-field intensity. The problem is thus reduced to the solution of Maxwell's equations, subject to a nonlocal boundary condition. Under the assumption that the dielectric medium is linear, homogeneous, and isotropic, Maxwell's equations reduce to the Helmholtz equation

$$(\nabla^2 + K^2)\mathbf{E}(\mathbf{r}) = 0, \qquad K = \begin{cases} \omega/c & \text{in air} \\ n_{\text{glass}}\omega/c & \text{in glass} \end{cases}, \tag{1}$$

where $\mathbf{E}(\mathbf{r})$ is the total electric field, K is the wave-vector amplitude, ω is the angular frequency of the incident light, c is the speed of light in air, and n_{glass} is the refractive index of the glass substrate and the sample (for simplicity and in view of the dominant influence of topographic features,[11] the refractive index of the sample is assumed to be equal to that of the glass substrate). This equation must be solved subject to the nonlocal boundary condition that

$$\mathbf{E}^i(r) + \frac{c}{4\pi\omega n_{\text{glass}}}\nabla\times\nabla \times \int_S \left[\mathbf{E}(\mathbf{r}')\frac{\partial G(\mathbf{r}|\mathbf{r}')}{\partial\hat{n}'} - G(\mathbf{r}|\mathbf{r}')\frac{\partial\mathbf{E}(\mathbf{r}')}{\partial\hat{n}'}\right]\mathrm{d}S' = 0\,, \tag{2}$$

$r \in$ air, where $\mathbf{E}^i(r)$ is the electric field in glass, G is Green's function, and $\hat{n}$ is a unit vector normal to the surface S. This is also known as the optical extinction theorem.[12] The theorem formally expresses

0146-9592/97/130955-03$10.00/0

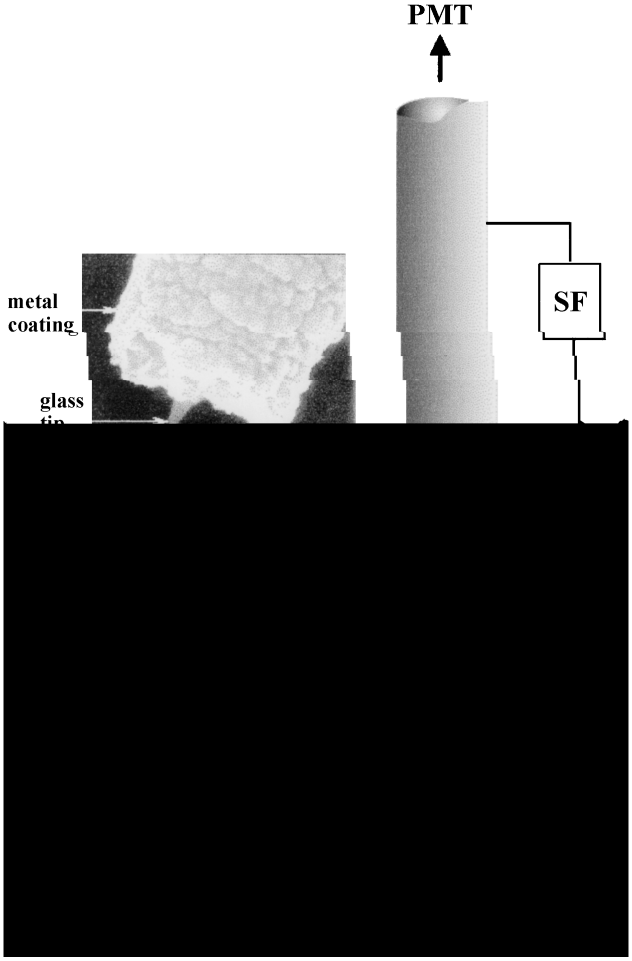

Fig. 1. Schematic diagram of the c-mode NOM experimental setup: LD, laser diode; $\lambda/2$, half-wavelength plate; PMT, photomultiplier tube; SF, shear-force control servo loop. When the shear-force control servo loop is locked the NOM setup runs in constant separation mode; otherwise it runs in constant-height mode. Inset: scanning electron microscope photograph of the fiber tip.

that if an electromagnetic wave electric vector $\mathbf{E}^i(r)$ is incident from glass upon air separated by a sample surface (S), it is canceled (extinguished) in the latter medium, giving rise to a new wave $[\mathbf{E}(\mathbf{r})]$. The electric field, Green's function, and their normal derivatives $(\partial/\partial n)$ are evaluated on the surface $(\mathbf{r}' \in S)$. When the sample height (h) is much less than the wavelength λ (the only case of practical interest), the electric field, Green's function, and their normal derivatives can be expressed as a power series of the sample height, allowing the problem to be solved in the small-perturbation limit by use of the field's angular spectrum representation (Rayleigh hypothesis). Under these assumptions, the near field is a vector sum of a large background field and a term containing the surface information filtered by propagation, translation, and diffraction factors. In the c-mode NOM operated in a constant-height mode (CHM) this model predicts both image inversion and edge enhancement.[6]

A biological specimen, a microtubule, was chosen as the subject of experimental investigation because of its well-identified nanometric size (with associated proteins, 25–30 nm in diameter and micrometers in length) and importance biologically. Its cylindrical shape allows for the investigation of directional and polarization effects, as the illumination direction can be varied with respect to the axis of the microtubule.

A schematic view of the experimental system is shown in Fig. 1. Focused light (linearly polarized) from a laser diode ($\lambda = 680$ nm) is incident upon the sample placed upon a glass prism. The polarization angle is controlled by means of a half-wave plate. A sharpened optical fiber is used to probe the evanescent field above the sample. This probe, fabricated by the two-step selective chemical etching method, was coated with a 200-nm gold film, which was subsequently etched away at the fiber tip to create a 30-nm aperture out of which the glass fiber protrudes.[1,13] (Fig. 1, inset). The light transmitted through the fiber is detected by a photomultiplier tube. Two coaxial peizo tubes are used. The outer tube supports a wagon upon which the prism and the sample are mounted and is used for both lateral scanning and Z positioning. For coarse vertical positioning it operates as a motor for a vertical piezoelectric inertial slider (slip–stick motion).[14] The inner tube holds and dithers the fiber when shear-force distance regulation is employed. A 1.3-μm laser diode–photodiode combination is used to monitor the fiber's vibration amplitude. To suppress air currents, the kinematic part of the system is enclosed in a case. All components are placed upon a vibration-damping stage.

The topographical layout of the sample was first determined by the shear-force technique to maintain a constant separation (~5 nm) between the fiber tip and the sample. In the shear-force (noncontact atomic force) image shown in Fig. 2(a) a microtubule with a height of 16 nm and an apparent width (FWHM) of 60–70 nm extends across the field of view. Having deter-

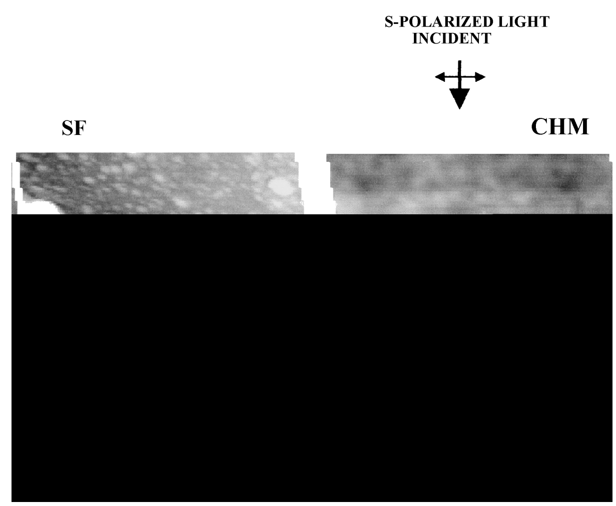

Fig. 2. Image of a microtubule (long and narrow) and a protein aggregate (round). (a) Topography of the 2 μm $\times$ 2 μm scan area obtained in shear-force mode. The microtubule and the aggregate are white. (b) Magnified optical image of the region highlighted in (a) taken in the CHM. Note the inversion of the optical image (dark) and the edge-enhancement effect in the images of both the microtubule and the protein aggregate. SF, shear force.

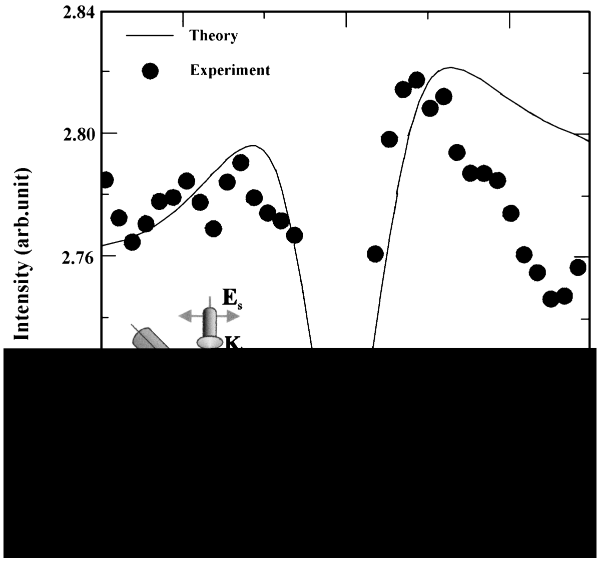

Fig. 3. Comparison of light intensity observed in passing over a microtubule in the CHM with theoretical calculations based on the optical extinction theorem. Inset: the geometry used in calculations based on the classical nonglobal model incorporating the optical extinction theorem. The refractive index of the microtubule is set equal to that of the glass substrate (1.5); $\varphi = 45°$ is an angle between the plane of the incident light and the microtubule's axis. wrt, With respect to.

mined the overall layout of the sample, we zero in on an isolated microtubule for a higher-resolution optical scan in the CHM to facilitate comparison with theory. (In the CHM the shear-force feedback loop is unlocked and the probe is kept at a constant height of ~30 nm from the surface of the prism.) Figure 2(b) shows the optical image of the area highlighted in Fig. 2(a) when s-polarized light was used for illumination of the sample with the direction of incidence shown in the figure. Comparing Figs. 2(a) and 2(b), we see that the optical image appears to be inverted and exhibits an edge-enhancement effect for both the microtubule and the nearby protein aggregate (round), in agreement with the qualitative predictions of the optical extinction theorem. As we have no independent determination of the size of the round protein aggregate that appears vividly in the center of the image, we limit our further quantitative discussion to the microtubule itself. A quantitative comparison is shown in Fig. 3. Here the observed light intensity (filled circles) is compared with the optical extinction theorem–based calculations (curve). Experimental data are taken along the line shown in Fig. 2(b). As illustrated in Fig. 3 (inset), for the purpose of calculation the microtubule is represented by a 30-nm-diameter half-cylinder with a refractive index of 1.5 placed upon a flat substrate of the same index. An s-polarized plane wave is incident upon the sample under total-internal-reflection conditions from below. The theoretical curve is obtained along the path depicted in Fig. 3 (inset) at a constant height from the substrate. We obtained the theoretical curve by adjusting the background level and the scan height, where the latter appears to be ~40 nm. The calculations seem to account accurately for the experimental results both for the apparent microtubule diameter (~40–50 nm) and in the observed asymmetry of the edge effect (the intensity is lower in the direction closest to the light source). It is interesting to note that such effects as image inversion and edge enhancement can be qualitatively understood with the aid of a simple quasi-electrostatic model (nonretardation limit).[6] Conversely, the effect of the edge asymmetry with respect to the direction of illumination requires the inclusion of the retarded Green function and thus indicates the limit where the electrostatic approach breaks down.

In summary, a detailed theoretical and experimental study of the imaging of a nanometer-sized dielectric sample by a c-mode NOM has been carried out and good quantitative agreement obtained. Application of nonglobal macroscopic theory to study the NOM image-formation mechanism for a small dielectric sample with a protruding fiber probe has proved to be a valid approach. In the future we expect to present a detailed comparison between theoretical calculations and experimental images for arbitrary polarization and direction of incident light.

We gratefully acknowledge the assistance of Shinichi Hisanaga of the Tokyo Institute of Technology and Hitoshi Tatsumi of Tokyo Medical and Dental University with the biological aspects of this research.

In Jesus' name.

References

1. See, for example, D. W. Pohl and D. Courjon, *Near Field Optics* (Kluwer, Dordrecht, The Netherlands, 1993); M. Ohtsu, J. Lightwave Technol. **13,** 1200 (1995).
2. O. J. F. Martin, C. Girard, and A. Dereux, Phys. Rev. Lett. **74,** 526 (1995).
3. K. Jang and W. Jhe, Opt. Lett. **21,** 236 (1996).
4. L. Novotny, D. W. Pohl, and P. Regli, J. Opt. Soc. Am. A **11,** 1768 (1994).
5. D. van Labeke and D. Barchiesi, J. Opt. Soc. Am. A **10,** 2193 (1993).
6. A. Zvyagin and M. Ohtsu, Opt. Commun. **133,** 328 (1997).
7. J. D. Jackson, *Classical Electrodynamics* (Wiley, New York, 1962), Chap. 16.
8. J. Cites, M. F. M. Sanghadasa, C. C. Sung, R. C. Reddick, R. J. Warmack, and T. L. Ferrell, J. Appl. Phys. **71,** 7 (1992).
9. J. C. Weeber, F. de Fornel, L. Salomon, E. Bourillot, P. Adam, and J. P. Goudonnet, Opt. Commun. **119,** 23 (1995).
10. J. C. Weeber, E. Bourillot, A. Dereux, J. P. Goudonnet, Y. Chen, and C. Girard, Phys. Rev. Lett. **77,** 5332 (1996).
11. O. J. F. Martin, C. Girard, and A. Dereux, J. Opt. Soc. Am. A **13,** 1801 (1996).
12. G. S. Agarwal, Phys. Rev. B **15,** 2371 (1977).
13. S. Mononobe, M. Naya, T. Saiki, and M. Ohtsu, Appl. Opt. **36,** 1496 (1997).
14. Ch. Renner, Ph. Niedermann, A. D. Kent, and Ø. Fisher, Rev. Sci. Instrum. **61,** 965 (1990).